2007 IEEE International Conference on
Robotics and Automation
Roma, Italy, 10-14 April 2007

Stability Proof of Biped Walking Control based on Point-Contact

Masahiro Doi and Yasuhisa Hasegawa, Takayuki Matsuno, Toshio Fukuda

Abstract— **As one of dynamics-based control of biped walking, some researchers presented the control method to take advantage of robot dynamics directly by use of point-contact state between a robot and the ground. We proposed Passive Dynamic Autonomous Control (PDAC) previously[13] as one of point-contact methods. PDAC expresses the robot dynamics as an 1-dimensional autonomous system based on the two concepts: 1) point-contact 2) Virtual Constraint (proposed by Grizzle and Westervelt *et al.*[8], [10]). We actually realized 3D dynamic walking by means of proposed method, however stability is not proved and the convergence domain is not clear. Thus, this paper finds the convergence domain of the previously proposed controller and proves the stability by the Liapunov Theory. Finally, the correctness of stability proof is confirmed by the numerical simulation.**

I. Introduction

In order to achieve natural and energy efficient biped walking, many control methods based on robot dynamics had been proposed up to this day. As one of such methods, some researchers presented the control methods to take advantage of robot dynamics directly by use of point-contact state between a robot and the ground[1]-[6]. Miura et al. produced the point-contact biped robot like stilt and realize dynamic walking by means of stabilizing control to change the configuration at foot-contact[7]. Kajita et al. proposed the control and stabilizing method based on the conserved quantity derived by designing the COG trajectory parallel to the ground[9]. Chevallereau presented the control to converge robot dynamics on optical trajectory by introducing the virtual time[12]. Grizzle and Westervelt et al. built the controller by use of the virtual holonomic constraint of joints named Virtual Constraint realize stable dynamic walking by means of the biped robot with a torso[8], [10], [11].

As one of point-contact methods, we proposed Passive Dynamic Autonomous Control (PDAC) previously[13]. PDAC expresses the robot dynamics as an 1-dimensional autonomous system based on the two concepts: 1) point-contact 2) Virtual Constraint (proposed by Grizzle and Westervelt *et al.*[8], [10]). We actually realized 3D dynamic walking by means of proposed method, however stability is not proved and the convergence domain is not clear. Thus, this paper finds the convergence domain of the previously proposed controller and proves the stability by the Liapunov Theory.

M. Doi is with the Department of Micro-Nano Systems Engineering, Nagoya University, JAPAN doi@robo.mein.nagoya-u.ac.jp

Y. Hasegawa is with the Graduate School of System and Information Engineering, University of Tsukuba, JAPAN hase@esys.tsukuba.ac.jp

T. Matsuno is with the Department of Intelligent Design Engineering, Toyama Prefectural University, JAPAN matsuno@pu-toyama.ac.jp

T. Fukuda is with the Department of Micro-Nano Systems Engineering, Nagoya University, JAPAN fukuda@mein.nagoya-u.ac.jp

II. Passive Dynamic Autonomous Control

A. Converged dynamics

As mentioned previously, PDAC is base on the two concepts, i.e. point-contact and *Virtual constraint*. Point-contact denotes that a robot contacts the ground at a point, that is, the first joint is passive. *Virtual constraint* was defined by Grizzle and Westervelt *et al.*[8], [10] as a set of holonomic constraints on the robot's actuated DoF parameterized by the robot's unactuated DoF. Assuming that PDAC is applied to the serial n-link rigid robot shown in Fig. 1, these two premises are expressed as follows:

$$\tau_1 = 0 \tag{1}$$

$$\begin{aligned}\boldsymbol{\Theta} &= [\theta_1, \theta_2, \cdots, \theta_n]^T = [f_1(\theta), f_2(\theta), \cdots, f_n(\theta)]^T \\ &:= \boldsymbol{f}(\theta)\end{aligned} \tag{2}$$

where θ is the angle around the contact point in the absolute

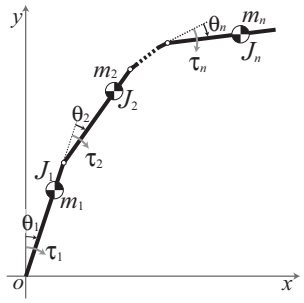

Fig. 1. Mechanical model of the serial n-link rigid robot. θ_i and τ_i are the angle and the torque of ith joint respectively. m_i and J_i are the mass and the moment of inertia of ith link respectively.

coordinate system, that is, $\theta_1 = f_1(\theta) = \theta$.

The dynamic equations of this model are given by

$$\frac{d}{dt}\left(\boldsymbol{M}(\boldsymbol{\Theta})\dot{\boldsymbol{\Theta}}\right) - \frac{1}{2}\frac{\partial}{\partial \boldsymbol{\Theta}}\left(\dot{\boldsymbol{\Theta}}^T \boldsymbol{M}(\boldsymbol{\Theta})\dot{\boldsymbol{\Theta}}\right) - G(\boldsymbol{\Theta}) = \boldsymbol{\tau} \tag{3}$$

where $\boldsymbol{M}(\boldsymbol{\Theta}) := [\boldsymbol{m}_1(\boldsymbol{\Theta})^T, \boldsymbol{m}_2(\boldsymbol{\Theta})^T, \cdots, \boldsymbol{m}_n(\boldsymbol{\Theta})^T]^T$, $\boldsymbol{\Theta} := [\theta_1, \theta_2, \cdots, \theta_n]^T$, $\boldsymbol{G}(\boldsymbol{\Theta}) := [G_1(\boldsymbol{\Theta}), G_2(\boldsymbol{\Theta}), \cdots, G_n(\boldsymbol{\Theta})]^T$, $\boldsymbol{\tau} := [\tau_1, \tau_2, \cdots, \tau_n]^T$, $\frac{\partial}{\partial \boldsymbol{\Theta}} = [\frac{\partial}{\partial \theta_1}, \frac{\partial}{\partial \theta_2}, \cdots, \frac{\partial}{\partial \theta_n}]^T$.

Since in this model the dynamic equation around the contact point has no term of the Coriolis force, it is given as

$$\frac{d}{dt}\left(\boldsymbol{m}_1(\boldsymbol{\Theta})^T\dot{\boldsymbol{\Theta}}\right) - G_1(\boldsymbol{\Theta}) = \tau_1 \tag{4}$$

By differentiating Eq. (2) with respect to time, the following equation is acquired,

$$\dot{\mathbf{\Theta}} = \frac{\partial \boldsymbol{f}(\theta)}{\partial \theta}\dot{\theta} = \left[\frac{\partial f_1(\theta)}{\partial \theta}, \frac{\partial f_2(\theta)}{\partial \theta}, \cdots, \frac{\partial f_n(\theta)}{\partial \theta}\right]^T \dot{\theta}. \quad (5)$$

Substituting Eq. (1), (2) and (5) into Eq. (3) yields the following dynamic equation,

$$\frac{d}{dt}\Big(M(\theta)\dot{\theta}\Big) = G(\theta) \quad (6)$$

where

$$M(\theta) := \boldsymbol{m}_1\Big(\boldsymbol{f}(\theta)\Big)^T \frac{d\boldsymbol{f}(\theta)}{d\theta} \quad (7)$$

$$G(\theta) := G_1\Big(\boldsymbol{f}(\theta)\Big). \quad (8)$$

By multiplying both sides of Eq. (6) by $M(\theta)\dot{\theta}$ and integrating with respect to time, the dynamics around the contact point is obtained as follows:

$$\int \Big(M(\theta)\dot{\theta}\Big)\frac{d}{dt}\Big(M(\theta)\dot{\theta}\Big)\,dt = \int M(\theta)G(\theta)\dot{\theta}\;d\theta \quad (9)$$

$$\iff \frac{1}{2}\Big(M(\theta)\dot{\theta}\Big)^2 = \int M(\theta)G(\theta)\;d\theta. \quad (10)$$

Therefore, the whole robot dynamics is expressed as the following 1-dimensional autonomous system (that is, the phase around contact point),

$$\dot{\theta} = \frac{1}{M(\theta)}\sqrt{2\int M(\theta)G(\theta)\;d\theta} \quad (11)$$

$$:= \frac{1}{M(\theta)}\sqrt{2\big(D(\theta)+C\big)} \quad (12)$$

$$:= F(\theta). \quad (13)$$

In this paper, we term Eq. (12) and (13) Converged dynamics.

B. PDAC Constant

Since Converged dynamics is autonomous, in addition, independent of time, it is considered as a conservative system. The integral constant in right side of Eq. (10), C, is a conserved quantity, which is termed PDAC Constant. Its value is decided according to the initial condition (as for biped walking, the state immediately after foot-contact), and kept constant during a cycle of motion. Thus, it is possible to stabilize the motion by keeping PDAC Constant at certain value.

The dimension of PDAC Constant is equal to the square of angular momentum and has relevance to it. As is well know, assuming that the robot shown in Fig. 1 resides in the horizontal plane, the angular momentum around contact point is conserved since there is no effect of gravitational force on the robot dynamics. In this condition, it is clear that $M(\theta)\dot{\theta}$(angular momentum)$= \sqrt{2C}$ from Eq. (12), since $G(\mathbf{\Theta}) = 0$ in Eq. (3) hence $D(\theta) = 0$. Note that, although angular momentum is not conserved in the condition which robot dynamics is affected by the gravitational force, PDAC Constant is conserved since it includes the effects of the gravitation. This paper demonstrates the convergency of PDAC Constant by the Lyapunov theory and proves the stability of walking.

III. 3D BIPED WALKING

In this section, control architecture of 3D biped walking is summarize simply.

A. Sagittal motion

1) 3-link model: For the sake of simplicity, in this paper upper body of a robot is not moved, hence the 3-link model as shown in Fig. 2 is employed. The dynamic equation of this model is described as Eq. (3) and that of the ankle joint of the stance leg is Eq. (4) where $n = 3$. The left side of Eq. (4) is described as follows:

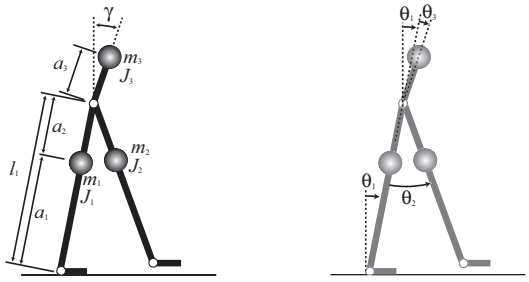

Fig. 2. 3-link model in the sagittal plane. m_i, J_i, l_i and a_i are the mass, the moment of inertia, the length of link and the distance from the joint to the link COG of link i respectively. γ is the angle of the forward tilting. In the right figure, θ_1, θ_2 and θ_3 are the ankle angle of the stance leg, the angle from the stance leg to the the swing leg, the relative angle between the stance-leg and trunk respectively.

$$\begin{aligned}
M_{11}(\Theta) &= J_1 + J_2 + J_3 + m_1a_1^2 + m_2l_1^2 + m_2a_2^2 \\
&\quad -2m_2a_2l_1\cos\theta_2 + m_3l_1^2 + m_3a_3^2 \\
&\quad +2m_3a_3l_1\cos\theta_3 \\
M_{12}(\Theta) &= -J_2 - m_2a_2^2 + m_2a_2l_1\cos\theta_2 \\
M_{13}(\Theta) &= J_3 + m_3a_3^2 + m_3a_3l_1\cos\theta_3 \\
G_1(\Theta) &= (m_1a_1 + m_2l_1 + m_3l_1)g\sin\theta_1 \\
&\quad +m_2ga_2\sin(\theta_2 - \theta_1) \\
&\quad +m_3ga_3\sin(\theta_1 + \theta_3)
\end{aligned}$$

where, $\mathbf{m}_1(\Theta) = [M_{11}(\Theta), M_{12}(\Theta), M_{13}(\Theta)]$.

2) Constraints of sagittal joints: Constraints are simply designed as follows:

- The angle of the torso is constant.
- The swing leg is symmetrical to the stance leg.

That is,

$$\theta_1 = f_1(\theta) = \theta \quad (14)$$

$$\theta_2 = f_2(\theta) = 2\theta \quad (15)$$

$$\theta_3 = f_3(\theta) = -\theta + \gamma \quad (16)$$

From Eq. (14)-(16) and (1), Eq. (6) is

$$\begin{aligned}
M_s(\theta) &= J_1 - J_2 + m_1a_1^2 + m_2l_1^2 - m_2a_2^2 \\
&\quad +m_3l_1^2 + m_3a_3l_1\cos(\gamma - \theta) \\
&:= E_1 + E_2\cos(\gamma - \theta) \quad (17) \\
G_s(\theta) &= (m_1a_1 + m_2l_1 + m_2a_2 + m_3l_1)g\sin\theta \\
&\quad +m_3ga_3\sin\gamma \\
&:= E_3 + E_4\sin\theta. \quad (18)
\end{aligned}$$

Thus,

$$\begin{aligned}\int M_s(\theta)G_s(\theta)d\theta &= \int \big(E_1 + E_2\cos(\gamma-\theta)\big)\big(E_3 + E_4\sin\theta\big)d\theta \\ &= E_2E_4\left(\frac{\sin\gamma}{2}\theta - \frac{\cos(2\theta-\gamma)}{4}\right) + E_1E_3\theta \\ &\quad + E_2E_3\sin(\theta-\gamma) - E_1E_4\cos\theta + C_s \\ &:= D_s(\theta) + C_s \qquad (19)\end{aligned}$$

where C_s is the integral constant, which is PDAC Constant of the sagittal motion. From Eq. (12), Converged dynamics in the sagittal plane is

$$\begin{aligned}\dot\theta &= \frac{1}{M_s(\theta)}\sqrt{2\big(D_s(\theta)+C_s\big)} \qquad (20)\\ &:= F_s(\theta). \qquad (21)\end{aligned}$$

Note that it is necessary that γ is decided so that $M_s(\theta) > 0$ in order to avoid singular point. Generally speaking, as for humanoid robots and biped robots, $E_1 > E_2$ since $l_1 > a_3$. Thus, we assume $M_s(\theta) > 0$ below.

3) Foot-contact model: Regarding foot-contact, it is assumed that the ground is perfectly inelastic collision and occurred for a moment similarly to previous works[8], [10], [2], [5]. That is, the angular momentum around the contact point is conserved before and after foot-contact.

Fig. 3 shows the angle and length of the inverted pendulum at foot-contact. Here, consider the foot-contact at the end of kth step, i.e. at the beginning of $k+1$th step. Denoting the angular velocity of ankle joint of the rear leg at foot-contact as $\dot\theta_e[k]$, the following equation is derived from Eq. (12):

$$\dot\theta_e[k] = \frac{1}{M_s(\theta_e[k])}\sqrt{2\big(D_s(\theta_e[k]) + C_s[k]\big)} \qquad (22)$$

where, $C_s[k]$ denotes PDAC Constant of kth step.

Since the torso angle is constant and COG is not rotated, the angular velocity of ankle joint of the fore leg at foot-contact, $P_i[k+1]$, is described as follows:

$$\begin{aligned}P_i[k+1] &= m_t l_e[k] l_i[k+1]\dot\theta_e[k] \\ &\quad \cdot\cos(\xi_e[k] + \xi_i[k+1]) \\ &= \frac{m_t l_e[k] l_i[k+1]\cos(\xi_e[k]+\xi_i[k+1])}{M_s(\theta_e[k])} \\ &\quad \cdot\sqrt{2\big(D_s(\theta_e[k]) + C_s[k]\big)} \\ &:= h[k]\sqrt{2\big(D_s(\theta_e[k]) + C_s[k]\big)} \qquad (23)\end{aligned}$$

where, $m_t = m_1 + m_2 + m_3$.

Since the angular velocity around the passive joint is

$$P = M_s(\theta)\dot\theta,$$

PDAC Constant after foot-contact, $C_s[k+1]$, is represented as

$$\begin{aligned}C_s[k+1] &= \frac{1}{2}P_i[k+1]^2 - D_s(\theta_i[k]) \\ &= h[k]^2 C_s[k] \\ &\quad + h[k]^2 D_s(\theta_e[k]) - D_s(\theta_i[k]) \\ &:= s_1[k]C_s[k] + s_2[k]. \qquad (24)\end{aligned}$$

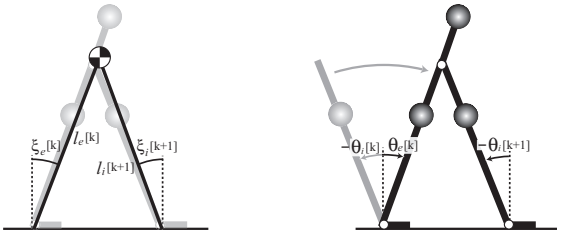

Fig. 3. Parameters at foot-contact. $l_e[k]$ and $\xi_e[k]$ are the length and inclination of the inverted pendulum which connects the ankle of support leg and robot COG before impact at the end of kth step. $l_i[k+1]$ and $\xi_i[k+1]$ are those after impact. $\theta_e[k]$ and $\theta_i[k+1]$ are the angles around the contact point before and after impact.

4) Sagittal motion period: In order to satisfy the condition of constant step-length, it is necessary to control the lateral motion so that lateral foot-contact period matches sagittal one. Since sagittal dynamics is expressed as an 1-dimensional autonomous dynamics, it is possible to calculate the sagittal foot-contact period by integrating sagittal Converged dynamics with time as follows:

$$T_s = \int_{i\theta^+}^{i+1\theta^-} \frac{1}{F_s(\theta)}\, d\theta. \qquad (25)$$

In next section, we design the lateral motion and build the controller satisfying the synchronization between lateral and sagittal motion.

B. Lateral motion control

1) Lateral motion: In this section, the lateral motion proposed previously in [13] is summarized briefly. In phase(A),

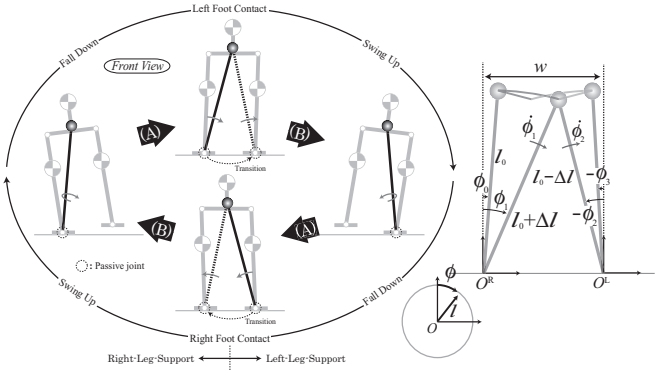

Fig. 4. Lateral motion (front view). The inverted pendulum falls off in phase(A) and swing up in phase(B). l and ϕ denote the length and the angle of an inverted pendulum. (l_0, ϕ_0) and $(l_0 + \Delta l, \phi_1)$ are the coordinates in Σ^R at the beginning and ending of phase (A), $(l_0 - \Delta l, \phi_2)$ and (l_0, ϕ_3) is that of Σ^L of phase (B) respectively. $\dot\phi_1$, $\dot\phi_2$ denotes the angular velocity at the end of phase (A) and at the beginning of phase (B)

a robot starts to turn over toward its swing-leg-side and

is accelerated by gravitation from the tilting position at a standstill on the stance-leg-side to foot-contact. In phase(B), after foot-contact, a robot is got up toward the tilting position at a standstill by the energy obtained in phase(A).

2) Constraint of lateral joints: The dynamic equation of an inverted pendulum is described as follows:

$$\frac{d}{dt}\left((ml^2+J)\dot{\phi}\right) = mgl\sin\phi + \tau, \tag{26}$$

where m, l, J, and ϕ are the mass, length, inertia moment, and angle of an inverted pendulum. τ is the torque around contact-point.

At first, we decide the *Virtual constraint*, that is, pendulum length l is described as the function of ϕ. It is clear that the right side of Eq. (37) can be integrated if $f(\phi)$ is a polynomial equation. Thus in this paper, $f(\phi)$ is decided as follows:

$$\begin{aligned} l &= f(\phi) && (27)\\ &= a\phi^2 + b\phi + c && (28)\end{aligned}$$

where a, b, and c are determined so as to satisfy the conditions described below. At first, the conditions of pendulum length at the beginning and ending of phase(A) and phase(B) introduce the following four equations:

$$\begin{aligned} f^A(\phi_0) &= l_0 && (29)\\ f^A(\phi_1) &= l_0 + \Delta l && (30)\\ f^B(-\phi_2) &= l_0 - \Delta l && (31)\\ f^B(-\phi_3) &= l_0 && (32)\end{aligned}$$

where upper-suffixes denote the differentiation of phases. In addition, the pendulum motion is designed so that the angular velocity of robot joints is not discontinuous, that is, the velocity along pendulum is zero,

$$\begin{aligned} \frac{\partial f^A}{\partial\phi}(\phi_1) &= 0 && (33)\\ \frac{\partial f^B}{\partial\phi}(-\phi_2) &= 0. && (34)\end{aligned}$$

From Eq. (29)-(34), a and b, c in each phase are decided.

From Eq. (27) and (1), Eq. (6) is

$$\begin{aligned} M_l &= mf(\phi)^2 + J && (35)\\ G_l &= mgf(\phi)\sin\phi. && (36)\end{aligned}$$

Thus, the phase around contact point (phase of passive joint) is obtained as below,

$$\begin{aligned} \dot{\phi} &= \frac{1}{M_l(\phi)}\sqrt{2\int M_l(\phi)G_l(\phi)d\phi} && (37)\\ &= \frac{1}{mf(\phi)^2+J}\sqrt{2\int mgf(\phi)\big(mf(\phi)^2+J\big)\sin\ d\phi}\\ &:= \frac{1}{M_l(\phi)}\sqrt{2\big(D_l(\phi)+C_l\big)}\\ &:= F(\phi) && (38)\end{aligned}$$

Finally, the value to lift up pelvis, Δl, is determined. Δl is necessary to be decided so that Eq. (38) satisfies the initial condition of phase(A) and the end condition of phase(B), that is,

$$\begin{aligned} & F_l^A(\phi_0) = F_l^B(-\phi_3) = 0\\ \Longleftrightarrow\quad & \frac{\sqrt{2\big(D_l^A(\phi_1) - D_l^A(\phi_0)\big)}}{M_l^A(\phi_1)}\cos(\phi_1+\phi_2) =\\ & \qquad\qquad \frac{\sqrt{2\big(D_l^B(-\phi_2) - D_l^B(-\phi_3)\big)}}{M_l^B(-\phi_2)} \end{aligned} \tag{39}$$

where upper suffixes denote the differentiation of phases. Δl is so small that it is possible to find the appropriate value satisfying Eq. (39) by use of the quadratic approximation.

3) Control of lateral period: Next we design the period controller of the lateral motion described in the previous subsection. The period of lateral motion is decided by the amplitude of pendulum motion, that is, the period is long if the amplitude is large and it is short if the amplitude is small. In this paper, the desired period is realized by controlling the lateral amplitude.

Assuming that the pendulum angle at the transition from phase(B) to phase(A) is ϕ_3, the motion period T can be found properly by the following calculation

$$\int_{-\phi_3}^{-\phi_2}\frac{1}{F_B(\phi)}d\phi + \int_{\phi_3}^{\phi_1}\frac{1}{F_A(\phi)}d\phi = T. \tag{40}$$

However, it is not easy to solve this equation for ϕ_3. The pendulum extension is so small that the desired amplitude is decided approximately by use of the model of inverted pendulum, length of which is not variable, as follows:

$$\phi_3 = \frac{\phi_c}{\cosh\left(\sqrt{\frac{g}{l_0}}\frac{T}{2}\right)} \tag{41}$$

where, ϕ_c is the pendulum angle in the standing posture, i.e. the pendulum angle at the foot-contact under the condition of $\Delta l = 0$.

IV. Stability proof of the sagittal motion

A. Constraint of constant step-length

As we presented in the previous work[13], the step-length is fixed at constant value, λ_d, in order to stabilize walking. Under such condition, it is clear that the following is held:

$$\theta_e[k] = -\theta_i[k] = \arcsin\left(\frac{\lambda_d}{2l_1}\right) := \theta_c = \text{const} \tag{42}$$

where $k \in \mathbf{N}$ and $0 \le \theta_c < \frac{\pi}{2}$. Since the torso angle, γ, is kept constant, $\xi_e[k]$ and $\xi_i[k]$, $l_e[k]$, $l_i[k]$ are also all constant similarly. Hence, in Eq. (23),

$$h[k] := H = \text{const}$$

is held. Besides, in Eq. (24),

$$\begin{aligned} s_1[k] &= h[k]^2 = H^2 := S_1 = \text{const}\\ s_2[k] &= h[k]^2 D_s(\theta_e[k]) - D_s(\theta_i[k])\\ &= H^2 D_s(\theta_c) - D_s(-\theta_c) := S_2 = \text{const}\end{aligned}$$

are also held.

B. Requisite to perform walking continuously

We consider the requisite to generate walking. In terms of practicality, let γ be $0 < \gamma < \frac{\pi}{2}$. In order to perform walking continuously, $\dot{\theta} > 0$ is required at all times. Considering $M_s(\theta) > 0$, this condition is equivalent to $P = M_s(\theta)\dot{\theta} > 0$. Since

$$\begin{aligned}\frac{dD_s(\theta)}{d\theta} &= M_s(\theta)G_s(\theta) \\ &= \big(E_1 + E_2\cos(\gamma-\theta)\big)\big(E_3 + E_4\sin\theta\big),\end{aligned}$$

and also since $E_3 > 0$ and $E_4 > 0$, in can be seen that $D_s(\theta)$ i.e. the angular velocity of passive joint, P, is minimum when

$$\theta = \arcsin\left(-\frac{E_3}{E_4}\right) := \hat{\theta}.$$

and that it decreases monotonically on $-\frac{\pi}{2} < \theta < \hat{\theta}$ and increases monotonically on $\hat{\theta} < \theta < \frac{\pi}{2}$. Since $\frac{1}{2}P^2 = D_s(\theta) + C_s$, the condition discussed above, $P > 0$, is described as below,

$$P > 0 \Longleftrightarrow C_s > -D_s(\hat{\theta}) := \hat{C}_s. \tag{43}$$

Therefore, from Eq. (24), the requisite to perform walking continuously is found as follows:

$$S_1\hat{C}_s + S_2 > \hat{C}_s. \tag{44}$$

Next, we argue the state that dynamics of walking is converged on a sole trajectory, i.e. the equilibrium state. On such condition, PDAC Constant of every steps is converged on constant value. That is,

$$C_s[k] = C_s[k+1] := C_s^*.$$

Hence, from Eq. (24),

$$\begin{aligned} & C_s^* = S_1C_s^* + S_2 \\ \Longleftrightarrow \quad & S_2 = C_s^*(1-S_1) \end{aligned} \tag{45}$$

is held. Substituting Eq. (45) into Eq. (44),

$$(1-S_1)(C_s^* - \hat{C}_s) > 0 \tag{46}$$

is obtained. From Eq. (43), it is clear that

$$C_s^* > \hat{C}_s. \tag{47}$$

From Eq. (46) and (47), the requisite to perform walking continuously, Eq. (44), is described as follows:

$$1 - S_1 > 0. \tag{48}$$

As for our robot (Gorilla Robot Ⅱ: Fig. 6, Table I), Eq. (48) is the range shown in Fig. 5. Although we assume $\gamma < \frac{\pi}{2}$ in Fig. 5, actual upper bound is decided according to the limitation of robot's specification such as the torque to swing a leg forward or to keep a torso angle at constant value.

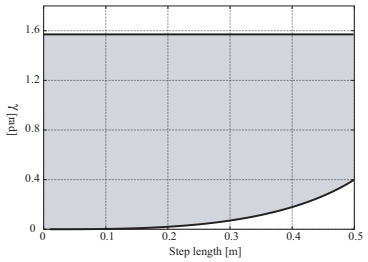

Fig. 5. Condition of θ and γ in order to generate continual walking

C. Proof of stability

Lastly, we prove the stability by Liapunov Theory using the conditions found above. The error between actual C_s and convergent value is defined as

$$\delta C_s := C_s^* - C_s. \tag{49}$$

The following positive definite function, V, is defined,

$$V = (\delta C_s)^2.$$

Since $V(0) = 0$ and $V > 0$ $(\delta C_s \neq 0)$, it is apparent that V is positive definite. From Eq. (24) and (45), (49), finite difference of V is

$$\begin{aligned}\Delta V &= V[k+1] - V[k] \\ &= \delta C_s[k+1]^2 - \delta C_s[k]^2 \\ &= (\delta C_s[k+1] + \delta C_s[k])(\delta C_s[k+1] - \delta C_s[k]) \\ &= -(2C_s^* - C_s[k+1] - C_s[k]) \\ &\qquad \cdot(C_s[k+1] - C_s[k]) \\ &= -(2C_s^* - S_1C_s[k] - S_2 - C_s[k]) \\ &\qquad \cdot(S_1C_s[k] + S_2 - C_s[k]) \\ &= -\big(2C_s^* - S_1C_s[k] - (1-S_1)C_s^* - C_s[k]\big) \\ &\qquad \cdot\big(S_1C_s[k] + (1-S_1)C_s^* - C_s[k]\big) \\ &= -(1+S_1)(1-S_1)(C_s^* - C_s[k])^2 \\ &= -(1+S_1)(1-S_1)\Delta C_s[k]^2. \end{aligned} \tag{50}$$

Since it is clear that $1 + S_1 = 1 + H^2 > 0$ from Eq. (43) and that $1 - S_1 > 0$ from Eq. (48), Eq. (50) is

$$\Delta V = 0 \quad (\delta C_s = 0). \tag{51}$$

In addition,

$$\Delta V < 0 \quad (\delta C_s \neq 0) \tag{52}$$

is held. From Eq. (51) and (52), ΔV is negative definite. Therefore, the equilibrium point, C_s^*, is asymptotically stable in the range shown in Fig. 5.

V. Simulation

In this section, stability proof described in the previous section is confirmed by the numerical simulation.

Fig. 7 is the phase portrait of θ and alteration in terms of time. From these figures, the convergency of the sagittal motion can be ascertained. Fig. 8 shows the snapshots of the simulation. On this simulation, step-length is 0.18[m], the torso angle is γ =0.035[rad].

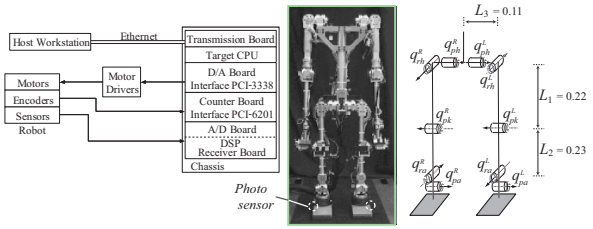

Fig. 6. Gorilla Robot Ⅱ (about 1.0[m] height, 22.0[kg] weight, 24 DOF)

TABLE I

LINK PARAMETERS OF GORILLA ROBOT Ⅱ

Mass[kg]	link1	m_1	2.618
	link2	m_2	3.451
	link3	m_3	15.143
COG position	link1	a_1	0.23
	link2	a_2	0.28
	link3	a_3	0.22
Moment of inertia	link1	J_1	0.042
	link2	J_2	0.070
	link3	J_3	0.047

Fig. 9 depicts the return maps of PDAC Constant and the angular velocity of passive joint at foot-contact. These figures show that the sagittal dynamics has a sole stable fixed point.

Finally, in order to confirm that the stability of the sagittal motion is independent of step-length, we perform the simulation of the various step-length. Fig. 10 is the graph of the return map of the angular velocity of passive joint at foot-contact v.s. step-length. From this figure, it can be confirmed that the sagittal dynamics is stable regardless of step-length.

VI. CONCLUSION

This paper proved the stability of sagittal motion designed previously by means of PDAC. The proof was conducted by the Liapunov Theory, and the convergence domain was also investigated. We confirmed the correctness of proof by numerical simulation. The proof in this paper handled

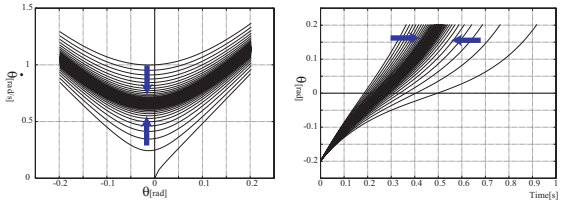

Fig. 7. Simulation results of sagittal stabilization. (Left) Phase portrait of the sagittal dynamics. (Right) θ trajectory vs. time.

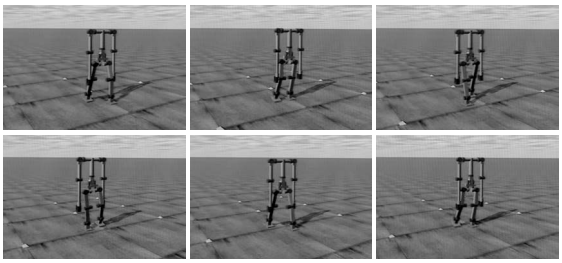

Fig. 8. Snapshot of the proposed walking

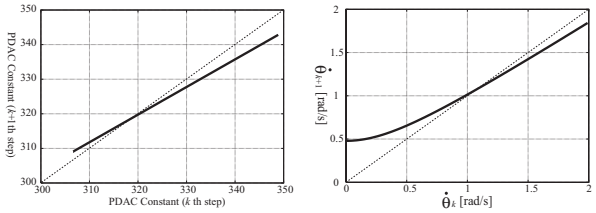

Fig. 9. Simulation results of sagittal stabilization. (Left) Return map of PDAC Constant. (Right) Return map of $\dot{\theta}$ at foot-contact.

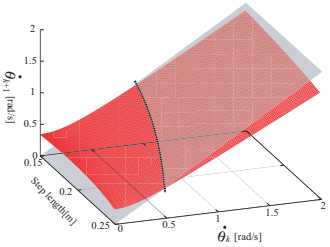

Fig. 10. Return map of $\dot{\theta}$ at foot-contact vs. step-length

the stability of 2D dynamics, thus the future work is to propose the walking controller achieving the stability of 3D dynamics, and prove the 3D stability of dynamic walking.

REFERENCES

[1] J. Nakanishi, J. Morimoto, G. Endo, G. Cheng, S. Schaal and M. Kawato, "A Framework for Learning Biped Locomotion with Dynamical Movement Primitives", The proceeding of IEEE-RAS/RSJ Int. Conf. on Humanoid Robots 2004, Paper no. 81.

[2] A. D. Kuo, "Stabilization of Lateral Motion in Passive Dynamic Walking", The International Journal of Robotics Research, Vol. 18, No. 9, September 1999, pp. 917-930.

[3] K. Ono, T. Furuichi and R. Takahashi, "Self-Excited Walking of a Biped Mechanism With Feet", The International Journal of Robotics Research, Vol. 23, No. 1, 2004, pp. 55-68.

[4] A. A. Grishin, A. M. Formal'sky, A. V. Lensky and S. V. Zhitomirsky "Dynamic Walking of a Vehicle With Two Telescopic Legs Controlled by Two Drives", The International Journal of Robotics Research, Vol. 13, No. 2, 1994, pp. 137-147

[5] A. Goswami, B. Espiau and A. Keramane, "Limit cycles in a passive compass gait biped and passivity-mimicking control laws", Autonomous Robots 4, 1997, pp.274-286, Kluwer Academic Publishers.

[6] J. Furusho and A. Sano, "Sensor-based Control of a Nine-Link Biped", The International Journal of Robotics Research, Vol. 9, No. 2, 1990, pp. 83-98.

[7] H. Miura and I. Shimoyama, "Dynamic Walking of a biped", The International Journal of Robotics Research, Vol. 3, No. 2, 1984, pp. 60-74.

[8] J. W. Grizzle, G. Abba and F. Plestan, "Asymptotically Stable Walking for Biped Robots: Analysis via Systems with Impulse Effects", IEEE Transaction on Automatic Control, Vol. 46, No. 1, 2001, pp. 56-64.

[9] S. Kajita, T. Yamaura and A. Kobayashi, "Dynamic walking control of a biped robot along a potential conserving orbit", IEEE Transactions on Robotics Automation, Vol. 8, No. 4, 1992, pp. 431-438.

[10] E. R. Westervelt, G. Buche and J. W. Grizzle, "Inducing Dynamically Stable Walking in an Underactuated Prototype Planar Biped", The proceeding of Int. Conf. Robotics and Automation, 2004, pp. 4234-4239.

[11] E. R. Westervelt, G. Buche and J. W. Grizzle, "Experimental Validation of a Framework for the Design of Controllers that Induce Stable Walking in Planar Bipeds", The International Journal of Robotics Research, Vol. 24, No. 6, 2004, pp. 559-582.

[12] C. Chevallereau, "Time-Scaling Control for an Underactuated Biped Robot", IEEE Transactions on Robotics Automation, Vol. 19, No. 2, 2003, pp. 362-368.

[13] M. Doi, Y. Hasegawa, T. Fukuda, "Passive Dynamic Autonomous Control of Bipedal Walking", The proceeding of IEEE-RAS/RSJ Int. Conf. on Humanoid Robots 2004, Vol. 2, pp. 811-829.